

Electronic Supplementary Information for:

Two Unique 8-quinolinato (q) Based One Dimensional Complexes $[\text{Fe}^{\text{II}}\text{Mn}^{\text{II}}(\text{q})_4 \cdot (\text{H}_2\text{O})_{0.25}]_n$ and $[\text{Mn}^{\text{II}}(\text{q})_2]_n$: Synthesis, Structures, and Magnetism

Bo Li,^a Jingping Zhang,^{*a} Yan Zhang,^b Shuxin Cui,^a Wenliang Li,^a Yu Wang^a and Xiaoying Zhang^a

^aFaculty of Chemistry, Northeast Normal University, Changchun 130024, China.

*e-mail: zhangjingping66@yahoo.cn; ^bDepartment of Physics, Peking University, Beijing 100871, China.

Contents:

1. **Experiments:** (1) Starting materials; (2) Syntheses.
2. **Infrared Spectroscopy.** *Fig. S1.*
3. **Elemental analyses** (C, H, N, and Metals).
4. **X-ray Crystallography:** (1) **Table S1.** Selected bond distances (Å) and bond angles (°) for **1**; (2) **Table S2.** Selected bond distances (Å) and bond angles (°) for **2**; *Figs. S2-S6.*
5. **Magnetic Measurements:** (1) Field dependent magnetization of **1** at 2 K in the range of 0–5 T, *Fig. S7.* (2) Field dependent magnetization of **2** at 2 K in the range of 0–5 T, *Fig. S8.* (3) FC/ZFC/REM curves for complex **2** under 100 Oe from 2 to 15 K, *Fig. S9.*
6. **Theoretical fitting**

Experiments.

1.1. Starting materials. All chemicals and solvents used for synthesis are at reagent grade without further purification. The starting materials are 50% $\text{Mn}(\text{NO}_3)_2$ water solution, $\text{K}_3[\text{Fe}(\text{CN})_6]$, $\text{Cr}(\text{NO}_3)_3 \cdot 9\text{H}_2\text{O}$, and 8-hydroxyquinoline.

1.2. Syntheses of complexes 1 and 2.

1.2.1 $[\text{FeMn}(\text{8-quinolinato})_4 \cdot (\text{H}_2\text{O})_{0.25}]_n$ (**1**): $\text{Mn}(\text{NO}_3)_2$ 50% water solution (0.1 ml, 0.3 mmol) and 8-hydroxyquinoline (29 mg, 0.2 mmol) in 5ml methanol (green) were poured together into the prepared mixture of $\text{K}_3\text{Fe}(\text{CN})_6$ (33 mg, 0.1 mmol) and $\text{Cr}(\text{NO}_3)_3 \cdot 9\text{H}_2\text{O}$ (80 mg, 0.2 mmol) in 10 ml water (pale green). Then the consequent brown suspension was moved into the Teflon-lined steel autoclave, heated at 453 K for 48 h, and then slowly cooled to ambient temperature. Tiny X-ray quality dark brown needlelike crystals were washed using distilled water and collected by filtration. Yield: 40% (based on metal ions). IR (cm^{-1}): 3431(m), 3041(m), 1572(s), 1495(s), 1465(s), 1386(s), 1321(s), 1107(s), 822(m), 729(m). $\text{C}_{36}\text{H}_{26}\text{Fe}_1\text{Mn}_1\text{N}_4\text{O}_5$ (705.4): calcd. C 61.24, H 3.69, N 7.94; found C 61.21, H 3.64, N 7.98.

1.2.2 $[\text{Mn}^{\text{II}}(\text{8-quinolinato})_2]_n$ (**2**): The identical procedures with **1** but different stoichiometric ratio 10:20:1:2 for $\text{Mn}(\text{NO}_3)_2$:q: $\text{K}_3\text{Fe}(\text{CN})_6$: $\text{Cr}(\text{NO}_3)_3 \cdot 9\text{H}_2\text{O}$ afforded yellow

needlelike crystals suitable for single crystal X-ray diffraction, which were washed using distilled water and collected by filtration. Yield: 30% (based on Mn ions). IR (cm^{-1}): 3041(m), 1572(s), 1495(s), 1466(s), 1386(s), 1320(s), 1107(s), 821(m), 729(m). $\text{C}_{18}\text{H}_{12}\text{Mn}_1\text{N}_2\text{O}_2$ (343.24): calcd. C 62.93, H 3.50, N 8.16; found C 62.91, H 3.52, N 8.15. Further syntheses of other 8-quinolinato based chain complexes containing different magnetic centers are under processing with this economical method.

2. Infrared Spectroscopy. The probable magnetic impurity derives from the *in-situ* PBA (the mixture of $\text{K}_3\text{Fe}(\text{CN})_6$ and $\text{Cr}(\text{NO}_3)_3 \cdot 9\text{H}_2\text{O}$) with a characteristic IR absorption band in the range of $2000\text{--}2200\text{ cm}^{-1}$ for CN^- groups, which is not observed in the IR spectra for both complexes, to a certain extent ruling out the magnetic impurity.

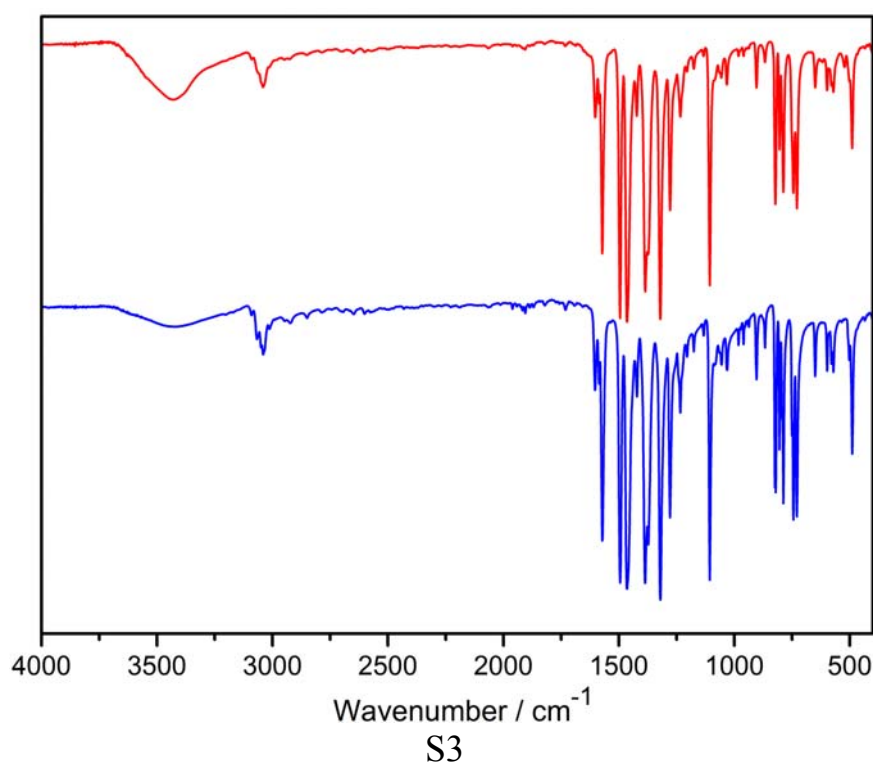


Fig. S1. The Infrared spectroscopy. The Infrared spectra of **1** (red solid line) and **2** (blue solid line) on KBr pellets were performed on a Bruker Vertex 70 FTIR instrument in the 4000-400 cm^{-1} region.

3. Elemental analyses (C, H, and N) were performed on a Perkin-Elmer 2400 CHN elemental analyzer. The metal contents and their molar ratio of complex **1** were characterized on the Varian 220FS Atomic Absorption System to be Fe and Mn ions in 1:1 ratio. The Fe and Mn ions in complex **1** are inferred according to their covalent radii and the bond lengths between metal ions and their corresponding nitrogen atoms. In consideration of bond lengths and the charge balance, Fe and Mn ions of complex **1** should be divalent, which is in accordance with the values (Mn1: 1.841, and Fe1: 1.988) calculated by the bond valence sum (BVS)² method. The metal content of complex **2** was also characterized on the Varian 220FS Atomic Absorption System to be Mn ions. The valance of Mn ions in complex **2** is calculated using BVS to be 1.891.

4. X-ray Crystallography. Single-crystal X-ray data sets of complexes **1** and **2** were collected on a Oxford Diffraction Gemini R Ultra detector diffractometer using the graphite monochromated Mo $K\alpha$ radiation ($\lambda = 0.71073 \text{ \AA}$) at 293(2) K. Intense data were collected by ω scan technique. The diffraction patterns for both complexes were indexed using CrysAlis³ software to obtain the unit cell parameters.

The structures were solved with the direct methods (SHELXS-97) and refined on F^2 by full-matrix least-squares (SHELXL-97).⁴

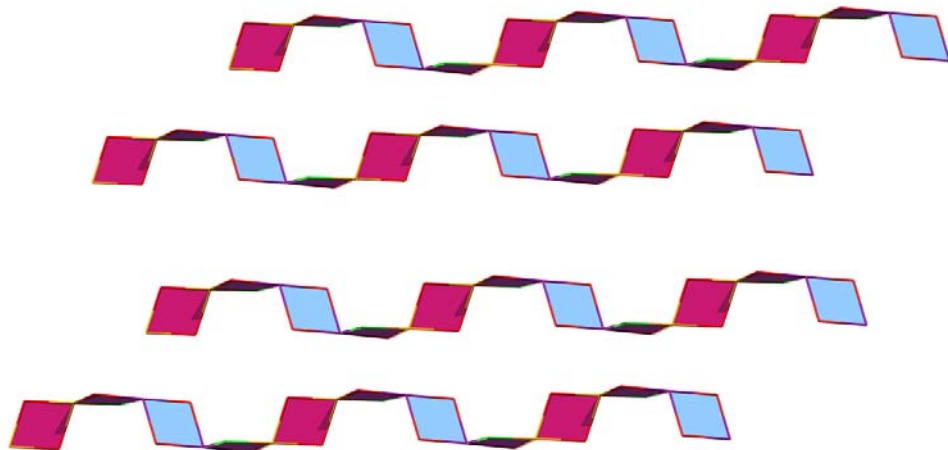


Fig. S2. Twisted ribbon like metal chain structures of complex 1. The representation of the four neighboring 1D chains in quadrangle: plum (double Fe1 and double O1), blue (double Mn1 and double O4), and purple (Fe1, Mn1, O2, and O3) colors. (vertexes: orange: iron; violet: manganese; red: oxygen O1, O3 and O4 and green: oxygen O2)

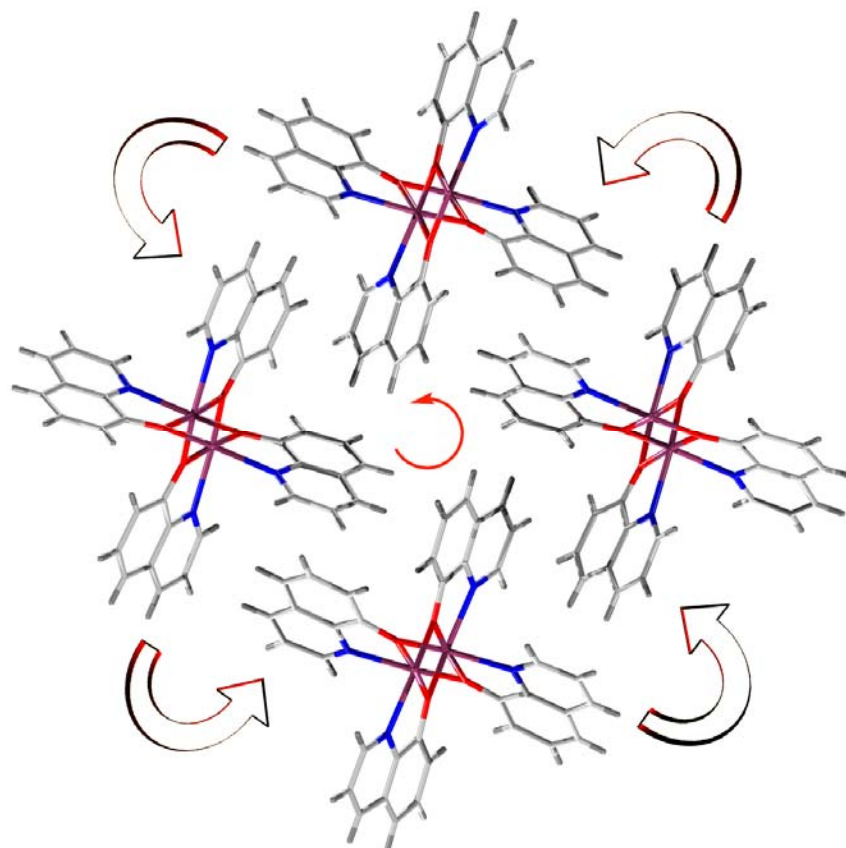


Fig. S3. Rotational four-blade propeller like structures of complex 2. The representation of the four neighboring 1D chains viewed down c axis: violet (Mn), red (O), blue (N), light-grey (C), and grey (H).

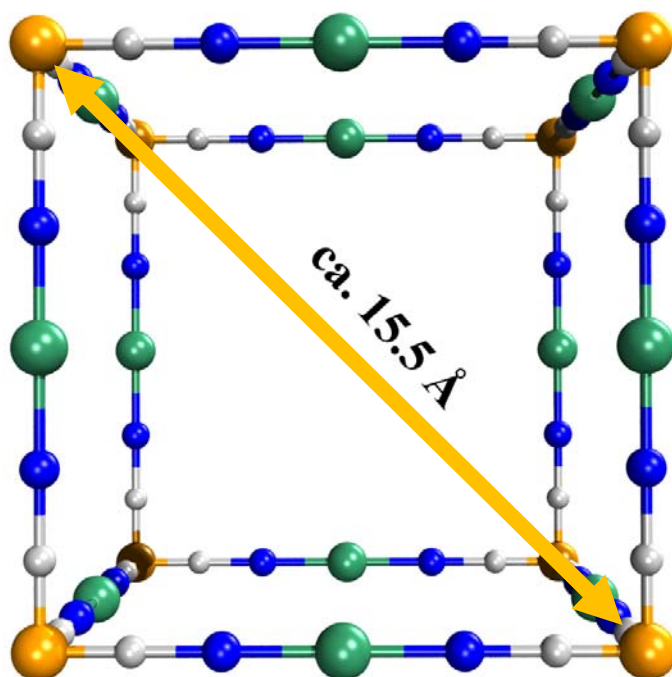


Fig. S4. The probable Cr-Fe Prussian blue framework. The representation of the Cr-Fe Prussian blue framework with a 15.5 Å diameter: green (Cr), orange (Fe), blue (N), and grey (C).

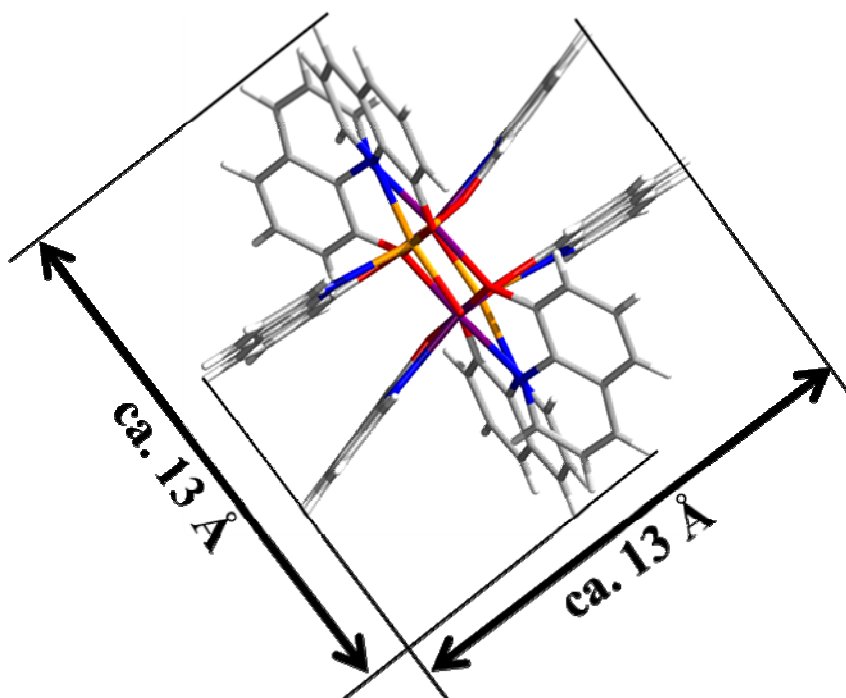


Fig. S5. The diameter of the 1D chain in complex 1. The representation of the 1D chain with a 13 Å diameter: violet (Mn), orange (Fe), red (O), blue (N), grey (C), and white (H).

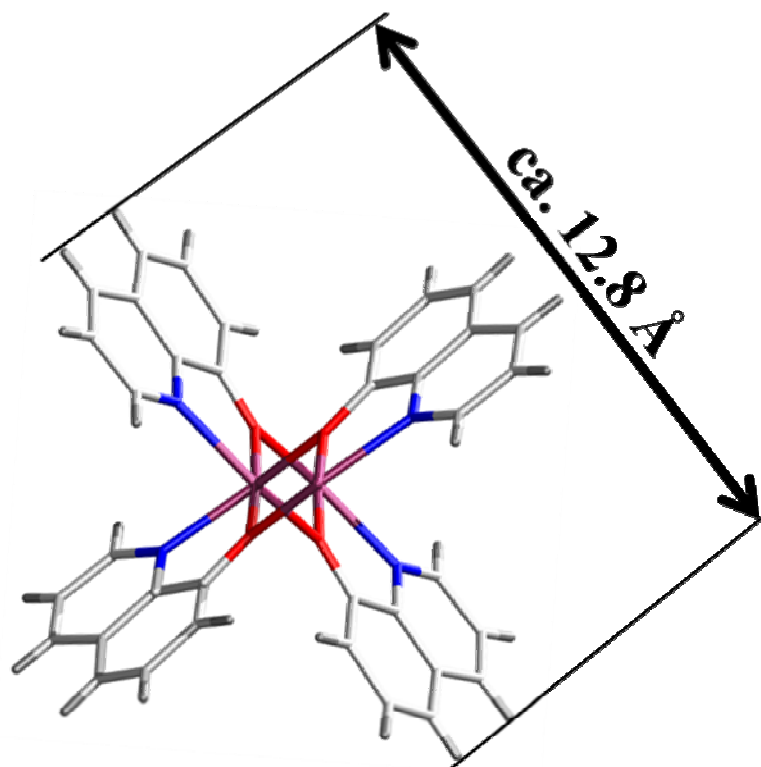


Fig. S6. The diameter of the 1D chain in complex 2. The representation of the 1D chain with a 12.8 Å diameter: violet (Mn), red (O), blue (N), grey (C), and white (H).

4.1. Table S1. Selected bond distances (Å) and bond angles (°) for complex 1.

Mn(1)-O(4)#1	2.136(3)	O(4)-Mn(1)-N(3)	111.14(13)
Mn(1)-O(2)	2.173(3)	O(3)-Mn(1)-N(3)	71.92(12)
Mn(1)-O(4)	2.194(3)	O(4)#1-Mn(1)-N(4)	142.62(12)
Mn(1)-O(3)	2.212(3)	O(2)-Mn(1)-N(4)	94.22(12)
Mn(1)-N(3)	2.316(4)	O(4)-Mn(1)-N(4)	72.29(12)
Mn(1)-N(4)	2.323(4)	O(3)-Mn(1)-N(4)	108.55(13)
Fe(1)-O(1)#2	2.126(3)	N(3)-Mn(1)-N(4)	84.74(14)
Fe(1)-O(3)	2.145(3)	O(1)#2-Fe(1)-O(3)	104.41(13)
Fe(1)-O(1)	2.194(3)	O(1)#2-Fe(1)-O(1)	74.32(11)
Fe(1)-O(2)	2.196(3)	O(3)-Fe(1)-O(1)	114.48(12)
Fe(1)-N(2)	2.236(4)	O(1)#2-Fe(1)-O(2)	106.08(11)
Fe(1)-N(1)	2.248(4)	O(3)-Fe(1)-O(2)	74.61(10)
O(1)-Fe(1)#2	2.126(3)	O(1)-Fe(1)-O(2)	170.69(12)
O(4)-Mn(1)#1	2.136(3)	O(1)#2-Fe(1)-N(2)	94.26(14)
O(4)#1-Mn(1)-O(2)	107.70(12)	O(3)-Fe(1)-N(2)	147.32(12)

O(4)#1-Mn(1)-O(4)	73.38(12)	O(1)-Fe(1)-N(2)	96.14(12)
O(2)-Mn(1)-O(4)	103.31(11)	O(2)-Fe(1)-N(2)	74.55(11)
O(4)#1-Mn(1)-O(3)	106.52(11)	O(1)#2-Fe(1)-N(1)	147.26(12)
O(2)-Mn(1)-O(3)	73.74(10)	O(3)-Fe(1)-N(1)	89.12(13)
O(4)-Mn(1)-O(3)	176.93(12)	O(1)-Fe(1)-N(1)	72.94(12)
O(4)#1-Mn(1)-N(3)	94.21(13)	O(2)-Fe(1)-N(1)	106.23(12)
O(2)-Mn(1)-N(3)	143.29(12)	N(2)-Fe(1)-N(1)	89.28(14)

#1 and #2 represent the symmetry transformations used to generate equivalent atoms: -x+1, -y+1, -z+1 and -x+1, -y, -z+1.

4.2. Table S2. Selected bond distances (Å) and bond angles (°) for complex 2.

Mn(1)-O(1)#1	2.150(2)	O(1)#1-Mn(1)-N(1)	142.53(7)
Mn(1)-O(2)	2.157(2)	O(2)-Mn(1)-N(1)	98.31(7)
Mn(1)-O(1)	2.216 (2)	O(1)-Mn(1)-N(1)	72.99(8)
Mn(1)-O(2)#2	2.234(2)	O(2)#2-Mn(1)-N(1)	105.84(7)
Mn(1)-N(2)#2	2.270(2)	N(2)#2-Mn(1)-N(1)	83.05(7)
Mn(1)-N(1)	2.272(2)	C(1)-N(1)-Mn(1)	127.6(2)
O(1)#1-Mn(1)-O(2)	107.57(7)	C(9)-N(1)-Mn(1)	114.46(18)
O(1)#1-Mn(1)-O(1)	72.51(7)	C(10)-N(2)-C(18)	118.3(2)
O(2)-Mn(1)-O(1)	111.54(6)	C(10)-N(2)-Mn(1)#2	126.84(19)
O(1)#1-Mn(1)-O(2)#2	107.34(6)	C(18)-N(2)-Mn(1)#2	114.63(17)
O(2)-Mn(1)-O(2)#2	73.06(7)	C(8)-O(1)-Mn(1)#1	134.71(14)
O(1)-Mn(1)-O(2)#2	175.32(7)	C(8)-O(1)-Mn(1)	117.29(15)
O(1)#1-Mn(1)-N(2)#2	90.49(7)	Mn(1)#1-O(1)-Mn(1)	107.49(7)
O(2)-Mn(1)-N(2)#2	144.85(7)	C(17)-O(2)-Mn(1)	136.99(15)
O(1)-Mn(1)-N(2)#2	102.49(7)	C(17)-O(2)-Mn(1)#2	116.00(15)
O(2)#2-Mn(1)-N(2)#2	72.83(7)	Mn(1)-O(2)-Mn(1)#2	106.94(7)

Symmetry transformations used to generate equivalent atoms: #1 -x+2, -y, -z and #2 -x+2, -y, -z+1

5. Magnetic Measurement.

Direct current (DC) Magnetic susceptibility measurements on polycrystalline samples of complexes **1** and **2** were carried out with Quantum Design SQUID MPMS XL-5 instruments in the temperature range 2–300 K and under the applied magnetic field of 1000 Oe. The

experimental susceptibilities were corrected for diamagnetism of the constituent atoms (Pascal's constants⁵).

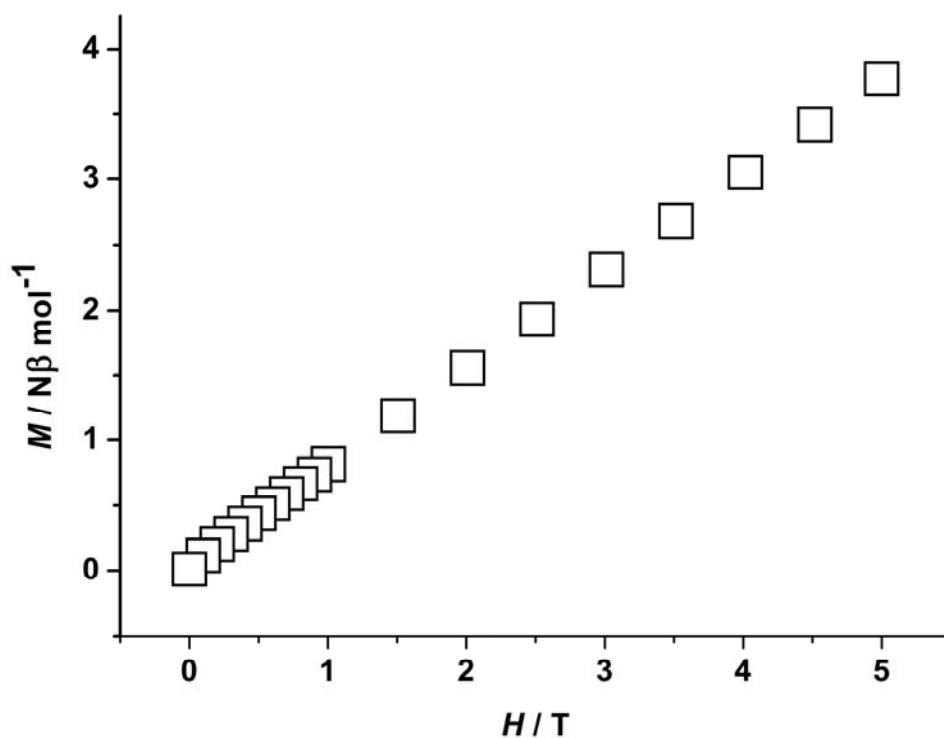


Fig. S7. Field dependent magnetization of 1. Field dependent magnetization measured at 2 K from 0 to 5 T.

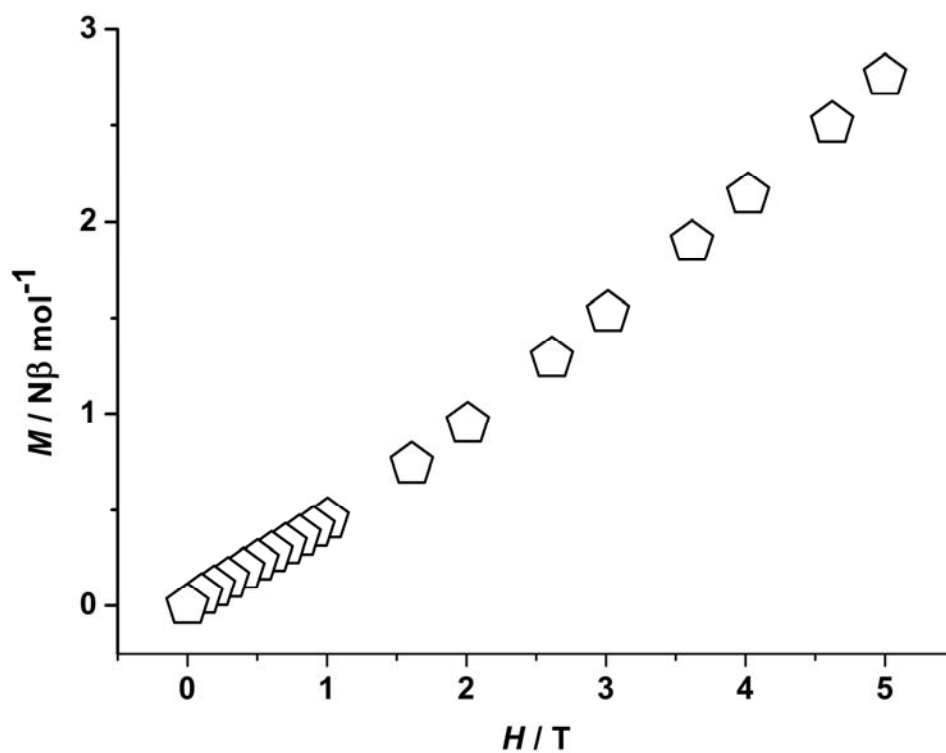


Fig. S8. Field dependent magnetization of 2. Field dependent magnetization measured at 2 K from 0 to 5 T.

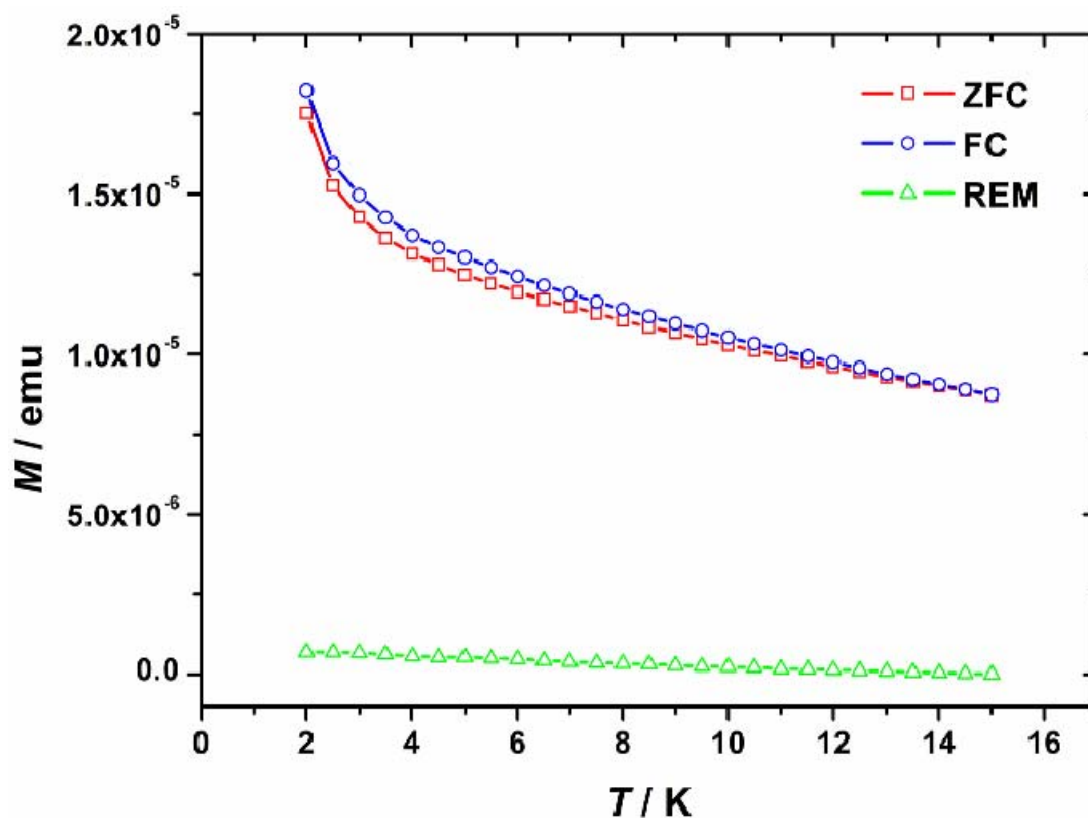


Fig. S9. FC/ZFC/REM curves under 100 Oe of 2. FC/ZFC/REM measurements were carried out using the polycrystalline sample under 100 Oe from 2 to 15 K. The decrease of the M value of the FC curve at low temperature, which is obvious under 1000 Oe, is not observed in the field of 100 Oe. This confirms that the decrease of the χ_m value at low temperature under 1000 Oe should be mainly owing to the field saturation effect.

6. Theoretical fitting

(1) Fisher model is suitable for fitting the infinite uniform homo-spin 1D magnetic chains, especially for the Mn^{II} ($S = 5/2$) containing ones.^{6a}

$$\chi^F = \frac{Ng^2\beta^2S(S+1)}{3kT} \frac{1+u}{1-u} \quad (\text{Fisher Model})$$

$$u = \coth\left[\frac{JS(S+1)}{kT}\right] - \left[\frac{kT}{JS(S+1)}\right]$$

(2) Drillon model is normally used for the infinite $\cdots\text{A-B-A-B}\cdots$ chain magnetic fitting. g^e and J^e represent the effective g-factors and interaction parameters, respectively.

$$\chi^D = \frac{N\beta^2}{3kT} \left[g^2 \frac{1+u}{1-u} + \delta^2 \frac{1-u}{1+u} \right] \quad (\text{Drillon Model})$$

$$g = (g_A^e + g_B^e)/2 \quad \delta = (g_A^e - g_B^e)/2$$

$$u = \coth\left[\frac{J^e}{kT}\right] - \left[\frac{kT}{J^e}\right]$$

$$g_A^e = g_A [S_A(S_A + 1)]^{1/2} \quad J^e = J [S_A(S_A + 1)S_B(S_B + 1)]^{1/2}$$

(3) The combination of Fisher and Drillon models to a new model used for the $\cdots\text{Fe-Fe-Mn-Mn}\cdots$ ($\cdots\text{A-A-B-B}\cdots$) type magnetic chains fitting (χ_{Fe}^F or χ_{Mn}^F represent the magnetic susceptibility taking the homo-spin Fe-Fe or Mn-Mn interaction into account, which is fitted using the Fisher model and $\chi_{\text{Fe-Mn}}^D$ represents the magnetic susceptibility taking the hetero-spin Fe-Mn interaction into account, which is fitted using the Drillon model).

$$\chi = 1/3\chi_{\text{Fe}}^F + 1/3\chi_{\text{Fe-Mn}}^D + 1/3\chi_{\text{Mn}}^F \quad (\text{Fisher-Drillon Model})$$

Equation S1:

$$A = \cosh(12.60875 * J_{\text{Mn}}/T) / \sinh(12.60875 * J_{\text{Mn}}/T) - (T/J_{\text{Mn}}/12.60875);$$

$$B = \cosh(8.646 * J_{\text{Fe}}/x) / \sinh(8.646 * J_{\text{Fe}}/T) - (T/J_{\text{Fe}}/8.646);$$

$$C = \cosh(10.441486 * J_{\text{Fe-Mn}}/T) / \sinh(10.441486 * J_{\text{Fe-Mn}}/T) - (T/J_{\text{Fe-Mn}}/10.441486);$$

$$\chi = 0.3646 * g_{\text{Mn}}^2 * (1+A)/(1-A)/T + 0.25 * g_{\text{Fe}}^2 * (1+B)/(1-B)/T + 0.0208 * ((2.958 * g_{\text{Mn}} + 2.449 * g_{\text{Fe}}) * (1+C)/(1-C) + (2.958 * g_{\text{Mn}} - 2.449 * g_{\text{Fe}}) * (1-C)/(1+C)) / T + \chi_T$$

IP;

References:

1. C. P. Berlinguette, A. Dragulescu-Andrasi, A. Sieber, H. U. Gdel, C. Achim, K. R. Dunbar, *J. Am. Chem. Soc.* **2005**, *127*, 6766.
2. M. O'Keefe, N. E. Brese, *J. Am. Chem. Soc.* **1991**, *113*, 3226.
3. Oxford Diffraction (2006). *CrysAlis*. Oxford Diffraction Ltd, Abingdon, Oxford, England.
4. G. M. Sheldrick, *SHELXS97* and *SHELXL97*; University of Göttingen: Germany, 1997.
5. O. Kahn, *Molecular Magnetism*; Wiley-VCH: New York, 1993.
6. (a) M. E. Fisher, *Am. J. Phys.* 1964, **32**, 343. (b) M. Drillon, E. Coronado, D. Beltran and R. Georges, *Chem. Phys.* 1983, **79**, 449.